Astron. Astrophys. 351, 1041–1050 (1999)

ASTRONOMY AND ASTROPHYSICS

Star count analysis based on the linear programming

H.G. Kim

Korea Astronomy Observatory, Taejon 305–348, Korea (hgkim@hanul.issa.re.kr)

Received 11 December 1998 / Accepted 18 August 1999

Abstract. A new, efficient method of deriving stellar number density distribution along a line of sight from star count data by using a *Linear Programming* technique is presented. The derived stellar number density distribution is further used to find a distance to a dark globule. In order to validate the algorithm, we select a dark globule Barnard 361 with known stellar number density distribution and distance. Our estimates of stellar density distribution and distance to the globule are in close agreement with previous results. The effects of the choice of the luminosity function and of the general extinction law on the resulting stellar density function are discussed. The algorithm is applied to star count data for a dark globule, LDN 400, whose distance is unknown. For this purpose, CCD observations were made toward LDN 400 in V band. The stellar number density distribution toward LDN 400 shows two prominent peaks at distances of 1.2 and 2.5 kpc. The density peaks roughly coincide with the Sagittarius arm and stellar density enhancement of OB stars. The stellar number density distribution is further used to derive the distance to LDN 400. When using the luminosity function of Gilmore & Reid (1983) and the Galaxy model of Bahcall & Soneira (1980), we found a distance to LDN 400 of 450 ± 50 pc and an extinction caused by the cloud of 2.4 ± 0.5 magnitudes in the V band.

Key words: Galaxy: structure – ISM: clouds – ISM: dust, extinction – ISM: individual objects: Barnard 361 – ISM: individual objects: LDN 400

1. Introduction

As the distance is one of the most fundamental quantities to characterize an interstellar cloud, many efforts have been done to derive it. The methods that have been frequently used are based on optical star counting, stellar photometry, stellar distances associated with that cloud, and kinematic distances, etc. Among them, the star count method described by Bok (1937) is particularly important to derive distance to a nearby dark cloud in the direction of the Galactic center or anticenter where the kinematic distance derived from Galactic rotation curve becomes highly uncertain.

Since the extinction due to the dust particles in a cloud would result in the decrease of the number of stars, one may derive the distance and extinction of an obscuring cloud by comparing the number of stars in an obscured field with that in an adjacent unobscured field. However, the actual application of the star count method to its fullest extent requires a large amount of effort and involves a variety of subjectiveness. Therefore only some simplified methods have been employed so far. The most widely employed one was to compare the observed star counts with those predicted by galaxy models (Duerr & Crain 1982; Magnani & de Vries 1986; Stüwe 1990) instead of finding stellar density distribution in the specific direction where the cloud resides. However, the actual stellar number density along a line of sight may vary from direction to direction, and may differ significantly from the galaxy model prediction. Therefore one must explicitly derive the stellar number density distribution along a specific line of sight for the fullest application of the star count method.

Hong & Sohn (1989) derived explicitly the stellar density distribution in finding distance to Barnard 361. However, they did not take into account the dependency of the luminosity function upon location in the Galaxy. Moreover they employed the classical approach in the derivation of stellar number density distribution where the $(m,\ \log\pi)$ table is used. This involves many tedious procedures and subjectiveness. One thus needs a more efficient method than the classical $(m,\ \log\pi)$ one.

In this paper, the star count analysis is improved in two aspects. First, we develop a new method of deriving explicitly the stellar number density distribution based on *Linear-Programming (LP)* technique of Press et al. (1986) in replacing the classical $(m,\ \log\pi)$ method. This remarkably reduces the computing time and subjectiveness. Second, we adopt χ^2-fitting method to remove the arbitrariness in determining the cloud distance and cloud extinction.

In Sect. 2, we explain the basic principles involved in the LP based star count method. After a brief description of the general formulation for star count method, detailed explanations of the LP algorithm for stellar density distribution and the LP algorithm for extinction and cloud distance will follow. In Sect. 3, test application of LP algorithm to a dark globule Barnard 361 is demonstrated. Effects of choice of luminosity function and size of the general extinction law on the resulting density function will also be described. In Sect. 4, we apply the LP algorithm to CCD data of a dark globule LDN 400. CCD observations and data reduction procedures are briefly de-

scribed. Subsequent application of the star count method using the modified Wolf diagram to find the distance to LDN 400 is also demonstrated.

2. Basic principles involved in the LP based star count analysis

2.1. General formulation for star counts

Suppose that a dark globule is located at a distance r_0 from the Sun and causes an extinction of E magnitudes. The number of stars $A(m)$ observed in an apparent magnitude interval $(m - 1/2)$ and $(m + 1/2)$ in the cloud direction over solid angle ω is given by

$$A(m) = \omega \int_0^\infty \Phi(M)\ D(r)\ r^2 dr, \tag{1}$$

where $\Phi(M)$ denotes the luminosity function with M being absolute magnitude, and $D(r)$ is the stellar number density distribution in units of the corresponding number density in the solar neighborhood. In Eq. (1), the apparent magnitude m is related to the absolute magnitude M, the general interstellar extinction $a(r)$, and the extinction due to the cloud E by

$$M = m + 5 - 5\log r - a(r) - \mu E,$$

where μ = 0 for the foreground stars ($r \leq r_0$) and μ = 1 for the background stars ($r > r_0$). The left hand side of Eq. (1) is obtained from the photometry of CCD image. Counts of the stars in a field of an arbitrary size are normalized to the corresponding numbers in $1^\circ \times 1^\circ$ field. The normalized distribution as a function of apparent magnitude $A(m)$ is usually presented in the form of $\log A(m)\ versus\ m$ curve. Such a curve is called the Wolf curve.

In order to solve Eq. (1) for cloud distance r_0 and the cloud extinction E, one must firstly know the stellar number density distribution $D(r)$. To derive $D(r)$, one needs to count stars in the unobscured field (E = 0) close to the program field which is called the reference field. The reference field should be carefully chosen so that the stellar number density distribution in it can be safely assumed to be the same as that in the program field. Similar to the case of the program field, the count at the reference field $A_{\rm r}(m)$ is given by

$$A_{\rm r}(m) = \omega \int_0^\infty \Phi(m + 5 - 5\log r - a(r))\ D(r)\ r^2 dr, \tag{2}$$

where M was replaced by $m + 5 - 5\log r - a(r)$. The integral equation [Eq. (2)] is then solved for $D(r)$ with a given luminosity function $\Phi(M)$ and a general extinction law $a(r)$.

Once $D(r)$ is obtained, Eq. (1) can be solved for the unknowns r_0 and E from the counts in the program field. The $\Phi(M)$ and $D(r)$ in the program field are assumed to be the same as those in the reference field.

2.2. Galaxy model for luminosity function

If the luminosity function $\Phi(M)$ is uniform over the whole Galaxy, Eq. (2) is enough to solve for $D(r)$. However, $\Phi(M)$ is generally known to decrease with increasing radius from Galactic center and distance from Galactic plane (Bahcall & Soneira 1980, hereafter BS; Jones et al. 1981). Therefore one should take into account the variation of the luminosity function with position in the Galaxy. This is particularly important if the source is at high Galactic latitude because the vertical scale height of stellar density is much shorter than the radial scale length.

A function $f(M; R, z)$ is introduced for the position dependency of the luminosity function in cylindrical coordinates. Eqs. (1) and (2) should thus be modified as

$$A_{(\rm r)}(m) = \omega \int_0^\infty \Phi(M) f(M; R, z)\ D(r)\ r^2 dr, \tag{3}$$

where $M = m + 5 - 5\log r - a(r) - \mu E$ for program field, and $M = m + 5 - 5\log r - a(r)$ for reference field. All other notations are the same as in Eqs. (1) and (2)

For the function $f(M; R, z)$, we adopt the galaxy model of BS which consists of disk and halo components. The halo component needs not to be considered here because the star count method is normally applied to a cloud well outside the central region of the Galaxy. The variation of luminosity function with position is then expressed approximately as

$$f(M; R, z) \sim \exp\left[-\frac{z}{H(M)} - \frac{(R - R_0)}{h}\right],$$

where R and z are distance and height in cylindrical coordinates. The scale length h of 3.5 kpc used by BS model is likely to be too large according to recent studies. Robin et al. (1992) found 2.5 kpc from optical study, and Ruphy et al. (1996) obtained even shorter value of 2.3 ± 0.2 kpc from near-infrared study. In this study a value of 2.5 kpc is taken for h. The distance of the Sun from Galactic center R_0 is taken as 8 kpc. For the scale height $H(M)$, the following relation from BS is used.

$$\begin{aligned}\left[\frac{H(M_{\rm B})}{\rm pc}\right] &= 90.0,\ M_{\rm B} < 2.8 \\ &= 73.4\ M_{\rm B} - 115.5,\ 2.8 < M_{\rm B} < 6.0 \\ &= 325.0,\ M_{\rm B} > 6.0\end{aligned}$$

$$\begin{aligned}\left[\frac{H(M_{\rm V})}{\rm pc}\right] &= 90.0,\ M_{\rm V} < 2.3 \\ &= 87.0\ M_{\rm V} - 110.1,\ 2.3 < M_{\rm V} < 5.0 \\ &= 325.0,\ M_{\rm V} > 6.0\end{aligned}$$

2.3. LP algorithm for density function

The integral in Eq. (3) for reference field is replaced by a summation over concentric shells centered on the Sun:

$$A_{\rm r}(m_{\rm k}) = \omega \sum_{i=1}^{i_{\max}} \Phi(M_{\rm k})\ f(M_{\rm k}; R_{\rm i}, z_{\rm i})\ D(r_{\rm i})\ r_{\rm i}^2\ \Delta r_{\rm i}, \tag{4}$$

with $M_{\rm k} = m_{\rm k} + 5 - 5\log r_{\rm i} - a(r_{\rm i})$. Here $\Delta r_{\rm i}$ is thickness of i-th shell, $R_{\rm i}$ and $z_{\rm i}$ are cylindrical coordinates of the center of the i-th cell. The concentric shells are taken uniformly from the Sun with radii,

$r_{\rm i} = 0.1, 0.2, 0.3, ..., 10.0$ kpc.

Since the stars at large distances are too faint to be detected with the CCD camera, it is in practice enough to extend the summation only up to $i_{\max} = 100$. The problem is to search for the most plausible stellar number density distribution, which best fits the observed Wolf curve in the reference field.

In order to transform Eq. (4) to an LP problem, a variable $R(m_{\rm k})$ is introduced which represents the fractional residual at each magnitude interval centered on $m_{\rm k}$ at reference field. The $R(m_{\rm k})$ is expressed as

$$R(m_{\rm k}) = 1 - A_{\rm r}^{\rm c}(m_{\rm k})/A_{\rm r}(m_{\rm k}),\ k = 1, 2, ..., k_{\max},$$

where $A_{\rm r}^{\rm c}(m_{\rm k})$ denotes the calculated count in unit magnitude interval centered on $m_{\rm k}$ at reference field as given by the right hand side of Eq. (4). The index k needs to be extended up to the limiting magnitude $m_{\rm k} = m_{\rm lim}$. The problem is to find a density function $D(r_{\rm i})$ that minimizes the weighted sum of absolute fractional residuals,

$$S = \sum_{k=1}^{k_{\max}} w_{\rm k} \left| R(m_{\rm k}) \right|. \tag{5}$$

The absolute expression in the above equation can be removed with suitable constraints. That is, the problem is equivalent to find $D(r_{\rm i})$ that minimizes the weighted sum of $R'(m_{\rm k})$'s,

$$\begin{aligned} S' &= \sum_{k=1}^{k_{\max}} w_{\rm k} R'(m_{\rm k}) \\ &= \sum_{k=1}^{k_{\max}} w_{\rm k} \left| 1 - A_{\rm r}^{\rm c}(m_{\rm k})/A_{\rm r}(m_{\rm k}) \right|, \end{aligned} \tag{6}$$

satisfying the following constraints:

$$A_{\rm r}^{\rm c}(m_{\rm k})/A_{\rm r}(m_{\rm k}) - R'(m_{\rm k}) \le 1\ (k = 1, 2, ..., k_{\max}), \tag{7}$$

$$A_{\rm r}^{\rm c}(m_{\rm k})/A_{\rm r}(m_{\rm k}) + R'(m_{\rm k}) \ge 1\ (k = 1, 2, ..., k_{\max}), \tag{8}$$

$$D(r_1) = 1, \tag{9}$$

$$D(r_{\rm i}) > 0\ (i = 2, 3, ..., i_{\max}), \tag{10}$$

where $w_{\rm k}$ is a suitably defined weighting function. Eq. (6) is the objective function or cost equation that we should minimize. The inequality constraints [Eqs. (7) and (8)] are the automatic constraints which are used to eliminate the absolute expression of fractional residuals in Eq. (5). The equality constraint [Eq. (9)] forces $D(r_1)$ in the first shell to stay at unity during iteration because $D(r_{\rm i})$ is expressed in units of the stellar number density in the solar neighborhood. The last constraint [Eq. (10)] prevents the density from being negative.

Any set of values $D(r_{\rm i})$ that satisfies all of the constraint equations [Eq. (7) - Eq. (10)] is called a feasible solution. A feasible solution that minimize the cost equation is called the optimal feasible solution. There is no limitation to the number of constraints as long as, at least, one feasible solution exists and the cost equation is bounded. Note that the inequality constraints [Eq. (7) and Eq. (8)] keep all $R'(m_{\rm k})$'s being non-negative automatically, and thereby keep the cost equation always positive and bounded. The program is written in FORTRAN-77 by using an IMSL package ZX0LP which is based on the revised simplex algorithm of Hadley (1962).

2.4. Modified Wolf diagram for cloud distance and extinction

Once $D(r)$ is obtained for the reference field as described in the above section, the next step is to find the cloud distance r_0 and the cloud extinction E. Assuming that $\Phi(M)$, $f(M_{\rm k}; R_{\rm i}, z_{\rm i})$ and $D(r)$ are the same as those for the reference field, Eq. (3) can be solved for the unknowns, r_0 and E, from the counts at the program field.

As for the reference field [Eq. (4)], we replace the integral by a summation. The computed count in the presence of a cloud, $A(m_{\rm k})$ is expressed in the same form as the right hand side of Eq. (4)

$$A(m_{\rm k}) = \omega \sum_{i=1}^{i_{\max}} \Phi(M_{\rm k})\ f(M_{\rm k}; R_{\rm i}, z_{\rm i})\ D(r_{\rm i})\ r_{\rm i}^2\ \Delta r_{\rm i}, \tag{11}$$

except that $M_{\rm k}$ is expressed as

$$M_{\rm k} = m_{\rm k} + 5 - 5 \log r_{\rm i} - a(r_{\rm i}) - \mu E.$$

The only difference of $M_{\rm k}$ in Eq. (11) from that of Eq. (4) is the term involving the parameter μ. In case E = 0 or $r_0 = \infty$, the situation is just the same as for reference field without cloud and $A(m_{\rm k})$ becomes identical to $A_{\rm r}(m_{\rm k})$.

In the classical star count method, the cloud distance r_0 and the cloud extinction E are determined from Eq. (11) by a trial-and-error method. That is, one may assign the trial values to r_0 and E and calculate the theoretical Wolf curve for the program field using Eq. (11). The calculated count $A^{\rm c}(m_{\rm k}; r_0, E)$ is then compared to the observed one $A(m_{\rm k})$. The values of r_0 and E are then renewed until the fit becomes satisfactory. In this scheme, however, it is difficult to find out which part contributes to E, and which part to r_0. Thus, We utilize a modified Wolf diagram of Hong & Sohn (1989) instead of the classical Wolf diagram. The modified Wolf diagram is $\Delta m\ versus\ m$ curve instead of $A(m)\ versus\ m$, where Δm is defined in such a way that the count at the program field $A(m)$ is equal to the count at the reference field $A_{\rm r}(m - \Delta m)$.

In this modified Wolf curve, the magnitude difference Δm increases with increasing magnitude in the bright part, and stays constant in the fainter part. This constant value is the extinction E caused by the cloud. Thus are can find the cloud extinction much easier using the modified Wolf diagram. Once the cloud extinction E is determined, only r_0 remains unknown. By comparing the observed modified Wolf curve with the constructed ones with several trial values of r_0, one can find the best fit cloud distance r_0.

Even when utilizing the modified Wolf curve, we still have some arbitrariness in the determination of both parameters, r_0 and E. We therefore introduced a less subjective, χ^2-fitting method where r_0 and E are determined simultaneously. We define

$$\chi_{\rm r}^2 = \sum_{k=1}^{k_{\max}} w_{\rm k} \cdot (\Delta m_{\rm k} - \Delta \tilde{m}_{\rm k})^2,$$

where $\Delta m_{\rm k}$ and $\Delta \tilde{m}_{\rm k}$ are defined in such a way that

$$A(m_{\rm k}) = A_{\rm r}(m_{\rm k} - \Delta m_{\rm k}),$$

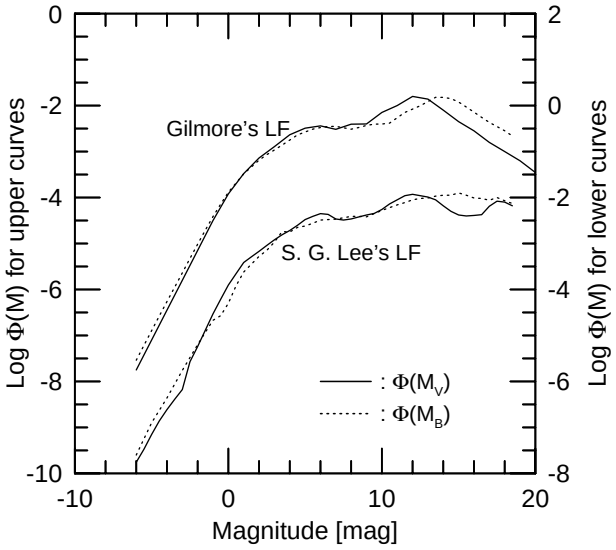

Fig. 1. The luminosity functions of Gilmore & Reid (1983) and Lee (1997/priv. comm.) are shown as a function of the absolute magnitude. Gilmore's luminosity function is a composite of three independent studies of Miller & Scalo (1979) for the range $-6 \leq M_{\rm V} < 2$, of Wielen (1974) for the range $2 \leq M_{\rm V} \leq 10$, and of Gilmore & Reid (1983) for the range $M_{\rm V} > 10$. The dotted line shows the blue luminosity function after the color correction from V to B.

and

$$A^{\rm c}(m_{\rm k}; r_0, E) = A_{\rm r}[m_{\rm k} - \Delta\tilde{m}_{\rm k}].$$

At first, series of modified theoretical Wolf curves are calculated for a hypothetical cloud with a given set of r_0 values with a fixed E. By comparing the theoretical Wolf curve at each set of r_0 and E with the observed one, we calculate a suitably defined error which is a weighted sum of deviations at each magnitude $m_{\rm k}$. Then the cloud extinction E is changed to the next value, and the same calculations is repeated. In this way, the weighted sum of deviations are obtained for every (r_0, E) grid point. In this scheme, the optimal cloud distance and extinction would be the (r_0, E) pair at which the weighted sum of deviations has its local minimum.

3. Test application to barnard 361

3.1. Effect of the luminosity function on D(r)

In order to apply the star count method to find a cloud distance, one should know which luminosity function is adequate for the region under study. One may ask how sensitively the stellar density function and the resulting distance to a cloud would depend on the choice of the luminosity function. To answer this question, we adopt two luminosity functions of Gilmore & Reid (1983) and Lee (1997/priv. comm.), and compare the resulting stellar density functions with each other. The luminosity functions are shown in Fig. 1.

Both luminosity functions were derived from disk stars in the solar neighborhood. Barnard 361 lies almost in the middle of the Galactic plane (l = 89.36°, b = −0.70°). Even though LDN 400 lies toward the Galactic center (l = 19.08°, b = 8.47°), its distance to the Sun looks small and its vertical distance from the Galactic plane is not so large. Thus the disk luminosity function is an appropriate choice for both Barnard 361 and LDN 400. For Barnard 361 the stars were counted in blue magnitudes. Thus the luminosity function must be transformed from $M_{\rm V}$ to $M_{\rm B}$ unit. Transformation was made using the color-magnitude relation tabulated by Lee (1985). The dotted line in Fig. 1 shows the blue luminosity function after the color correction from V to B.

The effect of the choice of the luminosity function on the resulting stellar density function is shown in Fig. 2 and Fig. 3. In both figures, panel (a) shows the resulting stellar number density distribution as a function of radial distance, and panel (b) shows the adjustment of the calculated Wolf curve(cross) to the observed one(open circle). For both calculations, a linear general interstellar extinction law with a proportional constant of 0.8 mag/kpc was assumed.

The stellar density distribution toward Barnard 361 revealed by the LP based star count method shows interesting results: a double peak structure of the density distribution at around 600 − 1200 pc and another at around 2.8 kpc. The first density enhancement is more prominent in the result using Gilmore's luminosity function, while it is barely resolved when using Lee's luminosity function. On the other hand, the result using Lee's luminosity function reveals secondary density peak around 2.8 kpc. The first density enhancement corresponds to the local Cygnus-Orion arm and the secondary one roughly coincides with the location of the Perseus arm inferred from the positions of young star clusters and H II regions (Mihalas & Binney 1981). Although the shapes and the positions are somewhat different from each other depending on the choice of the luminosity function, the double peak feature in the first density enhancement seems to be real since it appears in both figures.

In spite of the excellent fit seen in panel (b) in both figures, the resulting density functions are significantly different from each other. The explanation of the difference between the results with different luminosity functions would be out of the scope of this paper and deserves further study. From these test calculations, however, it is clear that the LP algorithm works well and the resulting stellar density function agrees well with the previous result of Hong & Sohn (1989). From the comparison of Figs. 2 and 3, we conclude that the choice of the luminosity function affects sensitively the resulting stellar density function. This fact indicates that our algorithm could be used as an indirect method to verify the luminosity function by applying it to a direction with known stellar density distribution.

3.2. Effect of the general extinction on D(r)

In the star count method, the general interstellar extinction law $a(r)$ should also be known $a\ priori$. However, it is very difficult to know the exact distribution of the interstellar extinction along a line of sight. Therefore, one often assumes the general interstellar extinction law as a linear function of radial distance with

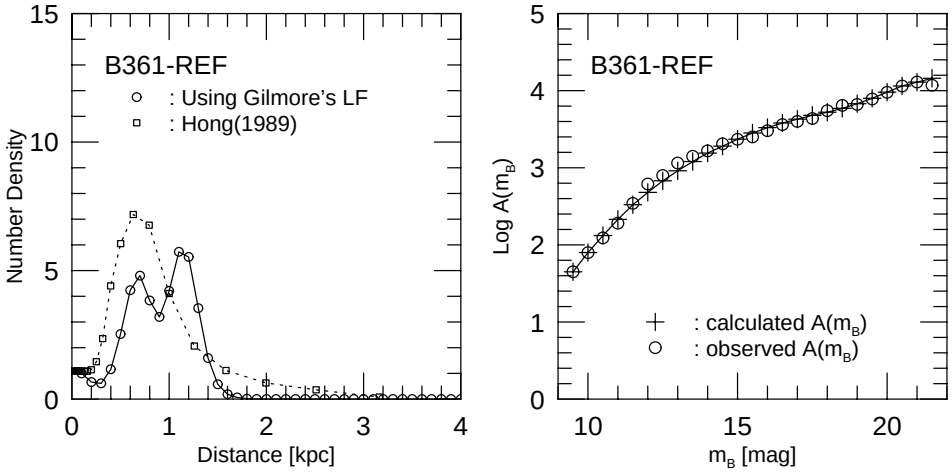

Fig. 2. Test application of LP based star count method to Barnard 361 using the luminosity function of Gilmore & Reid (1983). A linear general interstellar extinction law with a proportional constant of 0.8 mag/kpc was assumed. Left panel shows the resulting stellar density function which fits the observation best. Solid line shows the results obtained in this work. Dotted one shows the result of Hong & Sohn(1989) for comparison. Right panel shows the fit. The observed Wolf curve is denoted by open circles and the calculated one by crosses connected with solid line.

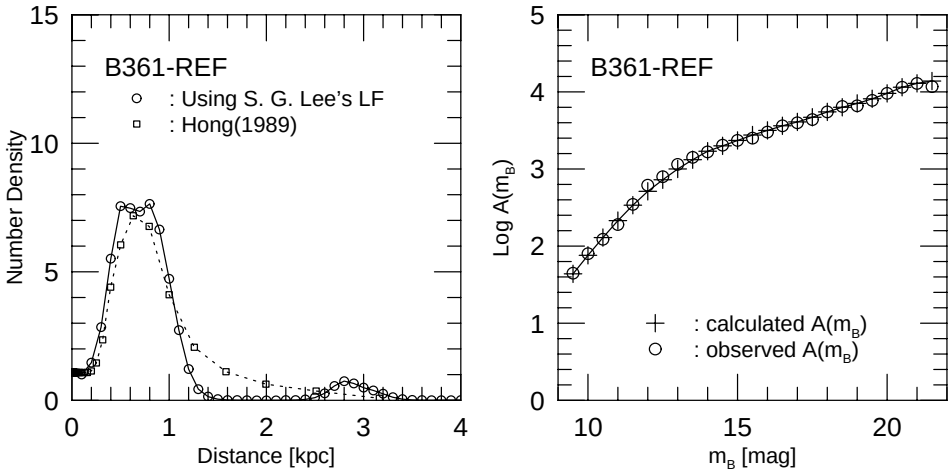

Fig. 3. Test application of LP based star count method to Barnard 361 using the luminosity function of Lee (1997/priv. comm.). A linear general interstellar extinction law with a proportional constant of 0.8 mag/kpc was assumed. All panels show the same thing as in Fig. 2.

a form $a(r) = k \cdot r$ for simplicity. The proportional constant k is also known to vary from direction to direction. The observed k-value determined by using the open clusters of known distance and extinction ranges from 0.5 to 1.0 mag/kpc (Alter & Ruprecht 1963; Ruprecht et al. 1981).

In order to examine the effect of the general interstellar extinction on the resulting stellar density function, we perform test calculations for a set of k = 0.5, 1.0, 1.5 and 2.0. The results are shown in Fig. 4 for both luminosity functions of Gilmore & Reid (1983) and Lee (1997/priv. comm.). For comparison, the result of Hong & Sohn (1989) is drawn in solid line.

As seen in Fig. 4, an increase in the proportional constant results in an increase of the stellar density function. This is natural because the number of stars should be increased to produce the same observed counts against the higher interstellar extinction. Additional trend in the spatial resolution can be noticed from these test calculations; As higher k-value is used, the resulting density structure tends to be smeared out. This tendency can also be attributed to the same reason. Another density peak can be seen at around 2.8 and 3.4 kpc with $k = 2.0$ and $k = 1.5$ when Gilmore's luminosity function is used. This may be attributed to the numerical errors because the stars at this distance contribute mostly to the faint end of the observations. This test calculation indicates that the index of general interstellar extinction law can also affect the resulting stellar density function significantly and thus should be determined carefully.

3.3. Determination of the distance to Barnard 361

Now, all the informations are gathered for determining the unknown parameters, r_0 and E. The procedure for determination of the cloud extinction E and the cloud distance r_0 using the modified theoretical Wolf curves is illustrated in Fig. 5. In the figure, several modified theoretical Wolf curves for a hypothetical cloud with a fixed E at five different r_0 are plotted. The faintest part of the modified theoretical Wolf diagram runs almost parallel to the magnitude axis, and Δm stays nearly constant at around 3.7 magnitudes. This value is the extinction caused by Barnard 361. Once the extinction is fixed, one may calculate theoretical Wolf curves with several trial values of cloud distance to find the best fit curve.

However, as seen in both figures it is very difficult to determine the best fit pair of (r_0, E) by eye fitting due to rather large scatters. We therefore introduced a less subjective method to determine r_0 and E simultaneously. Series of the modified theoretical Wolf curves are calculated with a hypothetical cloud on a given set of (r_0, E) grid points where the cloud distance r_0 ranges from 0 to 1200 pc by 50 pc step, and the cloud extinction

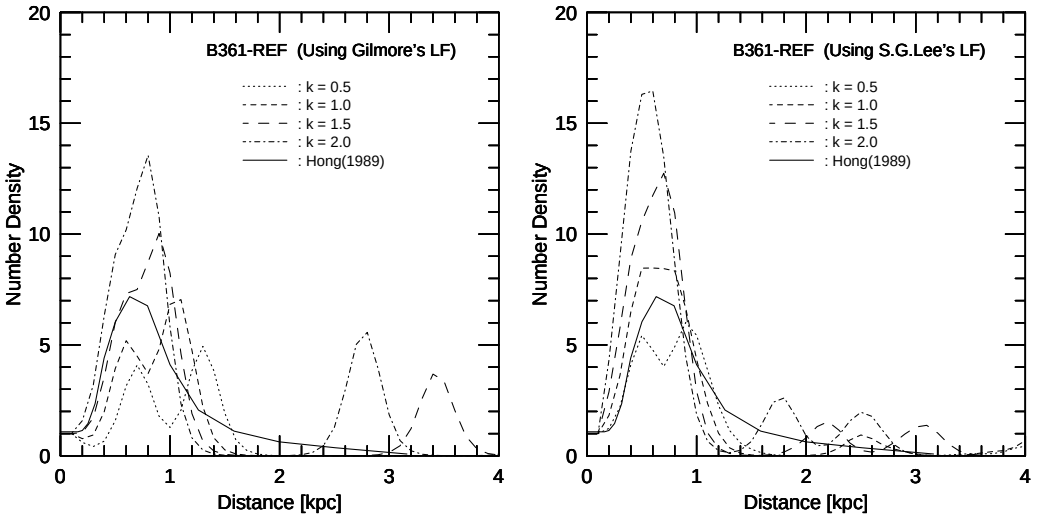

Fig. 4. Effect of the general extinction law on the resulting stellar density function for both luminosity functions. The general interstellar extinction law of a form $a(r) = k \cdot r$ was assumed. The solid line denotes the result of Hong & Sohn (1989) who use the proportional constant of 0.8 mag/kpc.

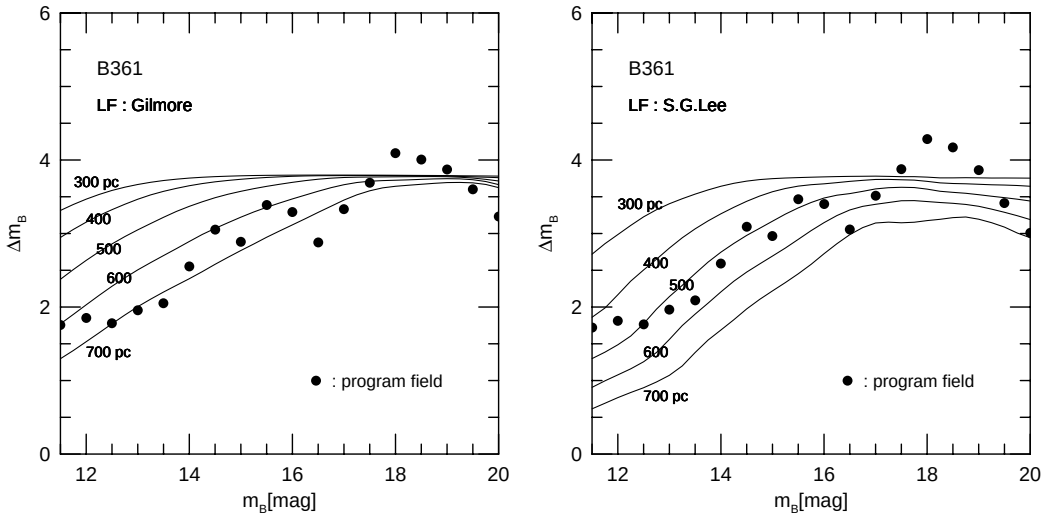

Fig. 5. Modified theoretical Wolf diagrams for Barnard 361. The luminosity functions of Gilmore & Reid (1983) and Lee (1997/priv. comm.) were used for comparison. Δm represents the horizontal distance in magnitude unit between the Wolf curves for the reference and program fields. Solid lines represent the modified theoretical Wolf curves for a hypothetical cloud with an extinction of 3.7 magnitudes in blue, at five different distances. Dots represent the observed Wolf curve for the program field of Barnard 361.

E from 0 to 10 magnitudes by 0.5 magnitude step. For each modified Wolf curve, we calculate an error which is defined as a weighted sum of vertical deviations of observed points from the theoretical curve.

The resulting errors are shown as contour plots in Fig. 6 for the luminosity function of Gilmore & Reid (1983) and Lee (1997/priv. comm.), respectively. One may find a well defined local minimum in each figure. From these figures, one can easily conclude that Barnard 361 has an extinction of 3.7 ± 0.5 magnitudes in blue. The distance, however, is different from each other depending on the luminosity function used: 630 ± 50 pc and 480 ± 50 pc for Gilmore's and Lee's luminosity function respectively. The result using Gilmore's luminosity function is in good agreement with that of Hong & Sohn (1989).

4. Application to LDN 400

4.1. CCD observations

While LDN 400 looks like a typical isolated dark globule with a single core in POSS print, it shows interesting features in radio and IRAS data. The ^{12}CO spectrum shows broad line width of about 3.5 km s^{-1} (Kim 1997), and an IRAS point source IRAS17526-0815 is located close to the core. These facts imply that LDN 400 may possibly be related to low mass star formation. The distance to LDN 400, however, has never been determined, and it is difficult to deduce its exact physical properties. We thus select this object to test our star count algorithm.

The CCD observations toward LDN 400 was made using the Bohyunsan Optical Astronomy Observatory (BOAO)'s 1.8 m

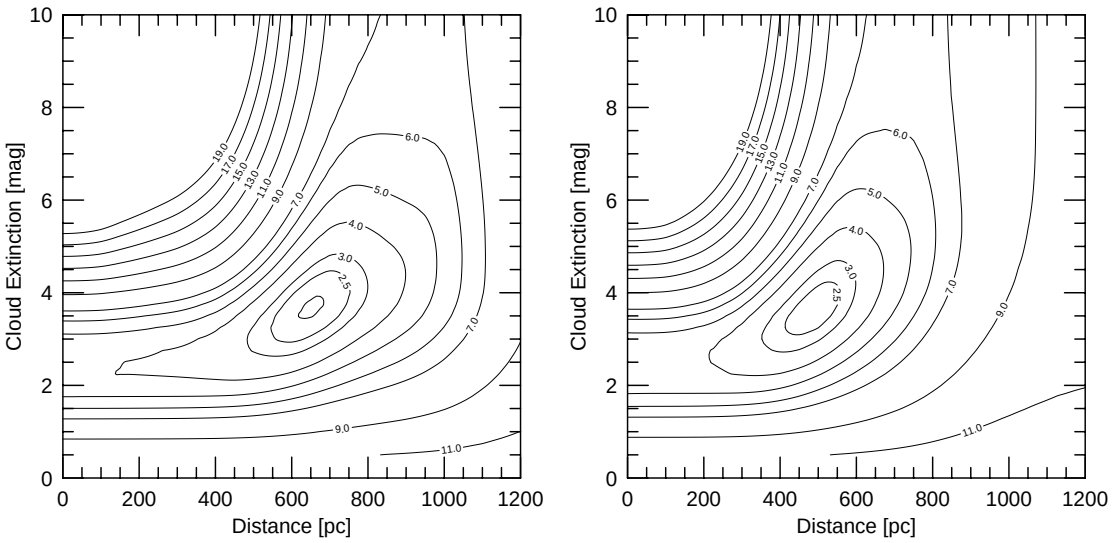

Fig. 6. Contour maps of weighted sum of deviations of the modified theoretical Wolf curves from that of the observed one for the program field of Barnard 361. The luminosity function of Gilmore & Reid (1983) was used for left panel, and that of Lee (1997/priv. comm.) for right one. The optimum point is found at r_0 = 630 pc and E = 3.7 mag and at r_0 = 480 pc and E = 3.7 mag, respectively.

Table 1. CCD observations summary

Field	Offset(′)†		Exposure(seconds)		Filter
	$\Delta\alpha$	$\Delta\delta$	long	short	
Program 1	0,	0	300	10	V
Program 2	10,	4	300	10	V
Reference 1	-20,	15	300	10	V
Reference 2	-20,	-20	300	10	V

† Offsets are in units of arcmin measured from LDN 400 center (α_{1950}, δ_{1950}) = ($17^{\rm h}\ 52^{\rm m}\ 48^{\rm s}$, -08° 15′ 00″).

telescope equipped with a CCD camera at the Ritchey-Chretien F/8 focus in May 1996. The CCD camera used was a Tektronics AR-coated 1024 × 1024 pixels array whose plate scale was 7.6″/mm. The sky area covered by a single frame is about 5.8′ × 5.8′. The seeing was about 2″ on average. We selected the reference fields by inspecting POSS prints so that they are close to the globule but well outside its boundary. In order to reduce the statistical errors, two fields for both program and reference fields were selected. Each frame was exposed twice; at first with long exposure and then with short exposure to prevent CCD from being saturated. Only the standard V filter was used for all exposures. Table 1 summarizes the CCD observations.

The preprocessings including bias subtraction and flat fielding were performed using the IRAF's CCDRED package. Stars were identified using DAOFIND task, and the instrumental magnitudes were obtained by using ALLSTAR task. The instrumental magnitudes were transformed to the standard visual magnitudes using the observations of several standard stars whose standard visual magnitudes are known. Five frames for standard stars were taken during the observations. The limiting apparent magnitude at 300 second exposure was about 21.5 magnitudes in V band.

Stars in each magnitude bin were counted and each count and convented into counts per square degree. The resulting Wolf

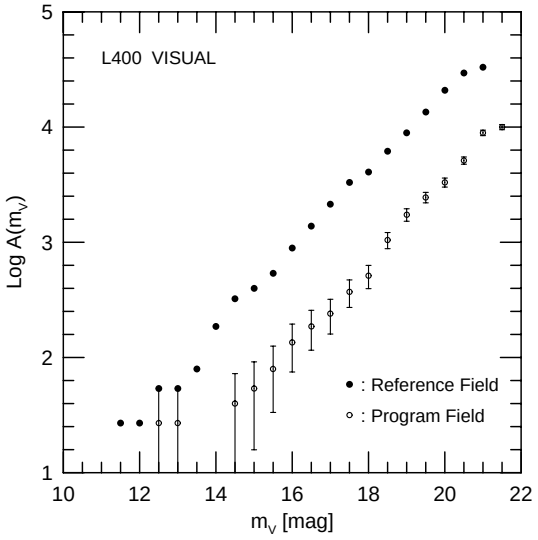

Fig. 7. Wolf diagrams for the program and reference fields of LDN 400. $A(m_{\rm V})$ is the number of stars in unit magnitude interval per square degree. The vertical bars on the open circles denote the statistical uncertainties involved in the counts. For convenience, error bars are denoted only on the counts at program field.

diagrams are shown in Fig. 7. The filled and open circles represent the counts in the reference and program fields, respectively. Length of the vertical bar on the open circle represents the uncertainty corresponding to the statistical fluctuation in the count assumed to follow the Poisson statistics.

4.2. Determination of k-value toward LDN 400

As discussed in Sect. 3.2, the general extinction law affects the resulting stellar density function significantly, and therefore must be determined carefully. To find k-value toward the

general direction of LDN 400, we tried to use the stellar photometry database in published catalog. The SKY2000 catalog maintained by CDS(Centre de Données astronomiques de Strasbourg) contains UBV photometric data of about 3×10^5 stars, and good for this purpose. But unfortunately, there are still not enough stars near LDN 400 with all the necessary data including apparent visual magnitude, (B-V) color and spectral class. We can only deduce roughly the k-value toward the general direction of LDN 400. We selected about 50 stars within 5 degrees of separation from the center of LDN 400. Among them, 20 variables and anomalous stars were excluded, and the remaining 30 stars were used for obtaining total extinction and distance from the Sun. Fig. 8 shows the total visual extinction versus distance. The ratio of total to selective extinction was taken as 3. The slope of the best fit line is 0.82 ± 0.18. Although this value was obtained for stars spread over several degrees wide, it may indicate that the general extinction toward LDN 400 may be lower than toward other directions. We thus take 0.8 mag/kpc for the k-value toward LDN 400.

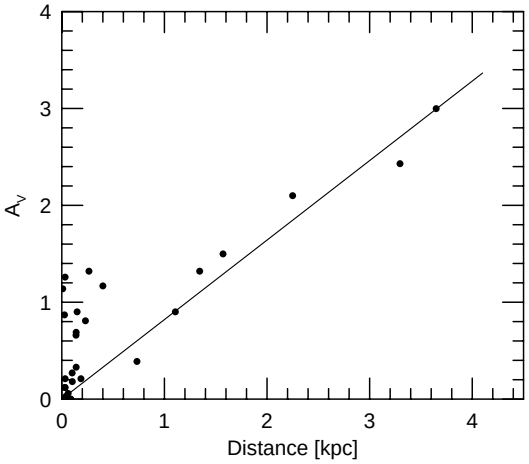

Fig. 8. Extinction $versus$ distance diagram for 30 stars toward the general direction of LDN 400. The solid line represents the best fit line passing through the origin. The slope is 0.82 ± 0.18.

4.3. Stellar density function toward LDN 400

Using the linear extinction law with k = 0.8 mag/kpc, we apply the LP program to the observed Wolf diagram at LDN 400 reference field to find stellar number density function along the line of sight. For comparison, we used both luminosity functions of Gilmore & Reid (1983) and Lee (1997/priv. comm.). The best fit results are shown in Figs. 9 and 10 for each luminosity function. Although the shape and location of innermost density enhancements are slightly different from each other, general trends resemble each other remarkably. The stellar number density distribution toward LDN 400 revealed by our LP based star count method shows two peaks of density enhancements. The first one at around 1.2 kpc corresponds roughly to the Sagittarius arm. The location of second peak at around 2.4–2.5 kpc coincides well with the location of the density enhancement of OB stars toward this direction (Schaifers & Voigt 1982).

Comparison of the stellar number density distribution with two different luminosity functions [Fig. 9 and Fig. 10] leads us to the following conclusions: (a) Toward LDN 400, the resulting stellar density function is not affected seriously by the selection of luminosity function. (b) Gilmore's luminosity function tends to put the location of the secondary density enhancement slightly farther from us than Lee's one. (c) Unlike the case of Barnard 361, the result obtained with both luminosity functions are surprisingly similar to each other, except a small ripple at the local and secondary density enhancements. Since the resulting density functions are similar to each other, we arbitrarily select Gilmore's luminosity function for deriving distance to LDN 400.

A note should be done on the relatively small number of bright stars toward LDN 400. Comparing Fig. 9 and Fig. 10 for LDN 400 with Figs. 2 and 3 for Barnard 361, one may remark that the stellar number density in the solar neighborhood toward LDN 400 ($l \sim 19.1°$) is much smaller than toward Barnard 361 ($l \sim 89.4°$). This seems to be real because the Sun is located at the inner edge of the local Cygnus-Orion arm and Barnard 361 is seen against this local arm.

4.4. Determination of distance to LDN 400

The stellar number density distribution obtained in the above section is used to determine the distance and extinction of a dark globule LDN 400. Procedures with both classical and modified Wolf diagrams are illustrated in Figs. 11 and 12, respectively. For this calculation, the luminosity function of Gilmore & Reid (1983) was used.

In the classical Wolf diagram shown in Fig. 11, the faint part of the theoretical Wolf curves with a hypothetical cloud runs almost parallel to that for reference field, and the horizontal distance in magnitude corresponds to the extinction of the hypothetical cloud. The variation of the cloud distance affects the shape of the theoretical Wolf curves only in the brighter part. Thus, one may find the cloud extinction by shifting calculated curves at reference field in left and right direction to fit the faintest side of the observed Wolf curve at the program field. Once the cloud extinction is fixed, only r_0 remains an unknown parameter. By varying r_0, we find the theoretical Wolf curve that best fits the observed curve as illustrated in the Fig. 11. This procedure can be done much easier if we use the modified Wolf diagram as shown in Fig. 12. In the case of LDN 400, the cloud extinction is found to be about 2.4 magnitudes in V, and the distance is about 400 pc when applying the classical or modified Wolf diagram.

In this scheme, one may have difficulty in determining r_0 and E, simultaneously. Thus we used the χ^2-fitting method described in the previous section. The result is shown as a contour plot in Fig. 13. In calculating χ^2, we adopted a weighting method which is reversely proportional to the visual magnitude. This is because the faint part of the modified Wolf curve of Fig. 12 runs almost parallel to the x-axis, and the bright part affects significantly the cloud distance. The selection of weighting method affects final distance and extinction by less than 10

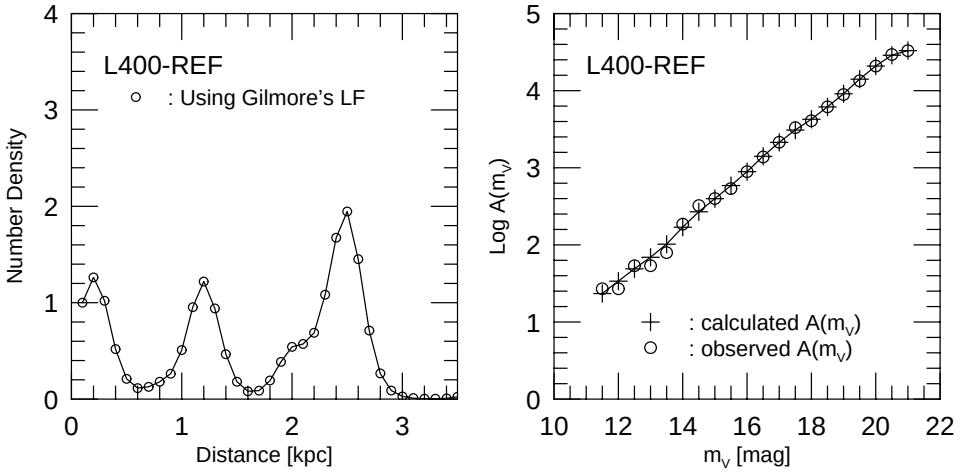

Fig. 9a and b. Application of LP based star count method to LDN 400 using the luminosity function of Gilmore & Reid (1983). A linear general interstellar extinction law with a proportional constant of 0.8 mag/kpc was assumed for this calculation. Panel **a** shows stellar density function which fits the observation best. Panel **b** shows the fit. The observed Wolf curve is denoted by open circles and the calculated one by crosses.

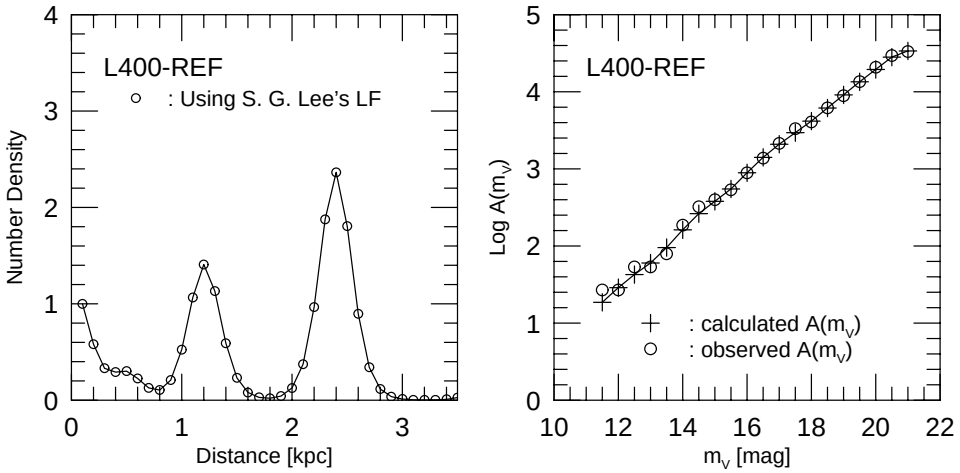

Fig. 10a and b. Application of LP based star count method to LDN 400 using the luminosity function of Lee (1997/priv. comm.). A linear general interstellar extinction law with a proportional constant of 0.8 mag/kpc was assumed for this calculation. All panels show the same thing as in Fig. 9.

per cent. From Fig. 13, we may easily conclude that LDN 400 is located at 450 $\pm$ 50 pc causing an extinction of 2.4 $\pm$ 0.5 magnitudes in visual.

5. Conclusions

A new method for finding stellar density function was developed on the basis of LP algorithm and applied to two dark globules Barnard 361 and LDN 400. Barnard 361 was selected for comparison purpose because for this globule an analysis with a classical star count method was done and the stellar density function is already known. Our analysis reveals that LP based star count method works well with high efficiency and is very powerful in finding stellar density function along a line of sight. The algorithm is applied to the dark globule LDN 400 whose distance has never been determined. It is found that the stellar density distribution toward LDN 400 shows two peaks at distances of 1.2 and 2.5 kpc, and the density function toward LDN 400 is not affected seriously by the choice of the luminosity function. The nearest density enhancement at around 1.2 kpc roughly corresponds to the Sagittarius arm. The location of the second peak at around 2.5 kpc coincides with a density enhancement of OB stars. All these facts imply that the LP based star count method produces reasonable results on the stellar number

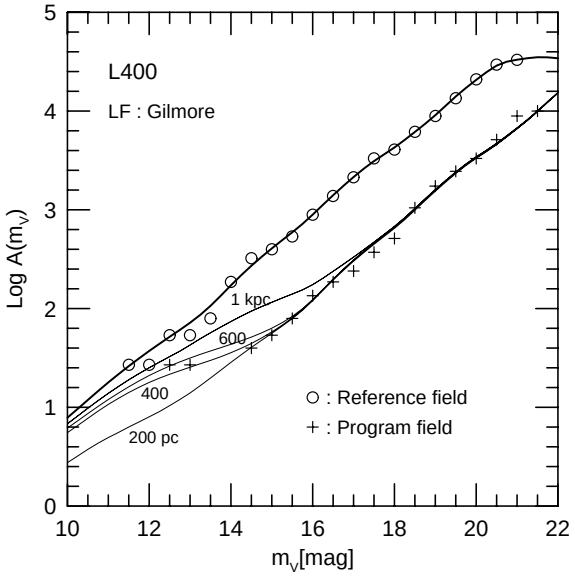

Fig. 11. Theoretical Wolf diagrams for a hypothetical cloud with a fixed extinction of E = 2.4 magnitudes at four different distances. The open circles denote the observed counts at reference field. Thick line represents the bet fit to the open circles. The crosses are the observed counts at program field. Thin lines are theoretical Wolf curves calculated with a hypothetical cloud at r_0 = 200, 400, 600 and 1000 pc.

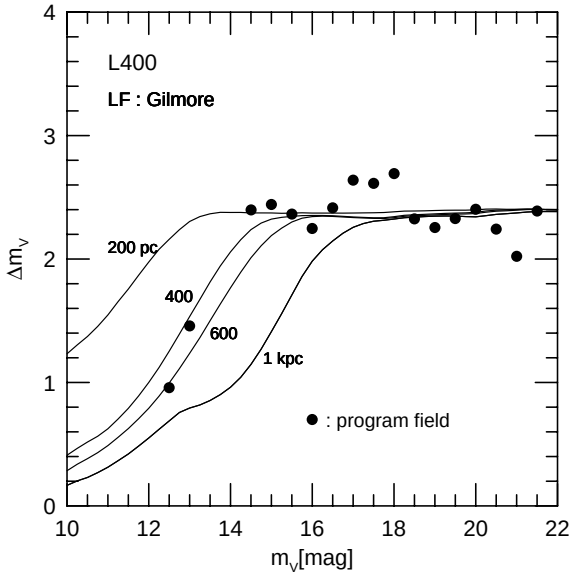

Fig. 12. Modified theoretical Wolf diagram for LDN 400. The luminosity function of Gilmore & Reid (1983) was used for this calculation. Δm represents the horizontal distance in magnitude unit between the Wolf curves for the reference and program fields. Solid lines represent the modified theoretical Wolf curves for a hypothetical cloud with an extinction of 2.4 magnitudes at four different distances. Dots represent the observed Wolf curve for the program field of LDN 400.

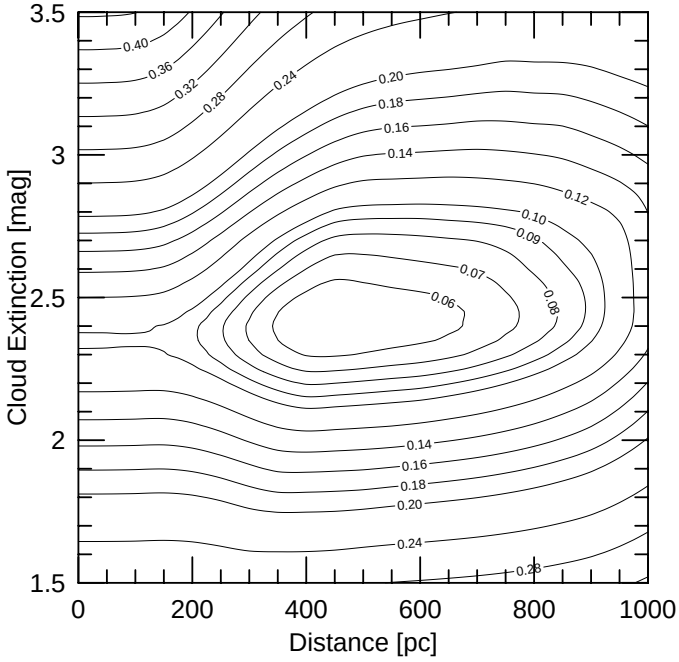

Fig. 13. Contour map of weighted sum of deviations of the modified theoretical Wolf curve from that of the observed one for the program field of LDN 400. The luminosity function of Gilmore & Reid (1983) was used for this calculation. The optimum point is found at r_0 = 450 pc and E = 2.4 mag.

density distribution from the Wolf curve at reference field. Subsequent application of the density function to the Wolf curve at program field determined the cloud extinction and distance of LDN 400. By utilizing the modified Wolf diagram, we found that LDN 400 is located at a distance of about 450 ± 50 pc from the Sun, and causes 2.4 ± 0.5 magnitudes of visual extinction.

Acknowledgements. I am grateful to BOAO staffs for the allocation of the observing time and kind supports during the observations, Dr. Hwankyung Sung for the CCD data reduction procedures. I also thank Dr. Jae Hoon Jung and Dr. Youngung Lee for valuable comments and careful reading of draft. I would like to express my sincere thanks to the referee Dr. N. Epchtein for helpful advice on this paper.

References

Alter G., Ruprecht J., 1963, in: The System of Open Star Cluster and Galaxy Atlas of Open Clusters, New York: Academic Press
Bahcall J. N., Soneira R. M., 1980, ApJS 44, 73
Bok B. J., 1937, in: The Distribution of the Stars in Space, University of Chicago Press, p. 124
Duerr R., Crain E. R., 1982, AJ 87, 408
Gilmore G., Reid N., 1983, MNRAS 202, 1025
Hadley G., 1962, in: Linear Programming, Massachusetts: Addison-Wesley, p. 207
Hong S. S., Sohn D. S., 1989, JKAS 22, 63
Jones T. J., Ashley M., Hyland A. R., Ruelas-Mayorga A, 1981, MNRAS 197, 413
Kim H. G., 1997, Ph. D. thesis, Seoul National University
Lee S.-W., 1985, in: Astronomical Observations and Data Analysis, Seoul: Min Eum Sa, p. 214
Magnani L., de Vries C. P., 1986, A&A 168, 271
Mihalas D., Binney J., 1981, in: Galactic Astronomy, 2nd ed., San Francisco: Freeman, p. 248
Miller G. E., Scalo J. M., 1979, ApJS 41, 513
Press W. H., Flannery B. P., Teukolsky S. A., Vetterling W. T., 1986, in: Numerical Recipes, Cambridge University Press, p. 312
Robin A. C., Crézé M., Mohan V., 1992, ApJ 400, L25
Ruphy S., Robin A. C., Epchtein N., et al., 1996, A&A 313, L21
Ruprecht J., Balazs B. A., White R. E., 1981, in: Catalogue of Star Clusters and Associations, Budapest: Akademiai Kiado
Schaifers K., Voigt H. H., 1982, in: Landolt-Börnstein, Heidelberg: Springer-Verlag Berlin, Vol. 2, Subvolume c, p. 191
Stüwe J. A., 1990, A&A 237, 188
Wielen R., 1974, in: Highlights of Astronomy, Reidel, Dordrecht, Holland, vol. 3, 395